

# Geometrical analysis on cap-shaped coils for power optimization of the vibration-based electromagnetic harvesting system

**Wan Hasbullah Mohd Isa, Khairul Fikri Muhammad, Ismail Mohd Khairuddin, Ismayuzri Ishak, Ahmad Razlan Yusoff**

Faculty of Manufacturing Engineering  
Universiti Malaysia Pahang

E-mail: wanhasbullah@ump.edu.my

**Abstract.** This paper presents the new form of coils for electromagnetic energy harvesting system based on topology optimization method which look-like a cap to maximize the power output. It could increase the number of magnetic flux linkage interception of a cylindrical permanent magnet which in this case is of 10mm diameter. Several coils with different geometrical properties have been build and tested on a vibration generator with frequency of 100Hz. The results showed that the coil with lowest number of winding transduced highest power output of 680 $\mu$ W while the highest number of windings generated highest voltage output of 0.16V.

## 1. Introduction

Autonomous sensors or sensor agents have been progressively popular due to certain cases where the energy sources are very limited or wired connection to the acquisition unit is not possible [1]. Batteries have been dominant electrical energy sources for these sensors but lately limited in some cases such as sizes, cyclic maintenance, disposition etc. because of the rapid miniaturisation of these devices.[2].

One of the attractive alternatives is energy scavenging or harvesting from potential ambient sources. Mechanical vibrations from various application domains such as machinery operations, human/machine movements etc. could become sustainable power sources [3]. Converting the energy from mechanical into electrical form could be done in either of combination of electromagnetic [4], piezoelectric [5] and/or electrostatic [6] transducers.

Electromagnetic transduction is based on Faraday's law by means of moving an internal mass across magnetic flux in a close loop of wire. Commonly a magnet is moved relative to a coil to harvest electrical energy. Therefore, a lot of magnet-coil architectures have been experimented in order to gain most electrical output from a vibrational source. In our study the system is based on cylindrical permanent magnet only.

Spreemann has tested several architectures of electromagnetic coupling based on a cylindrical magnet and found that configuration of coil underlying a magnet would produce most power output [7]. Using topology optimization approach to maximize the generated power output from the vibrating mechanical energy based on a cylindrical permanent magnet, a new proposed form of coil which look like a cap that enclosed more magnetic flux linkage in a limited construction boundary has been introduced [8].

The objective of this study is to analyse and compare seven topology-optimized coils with different geometrical properties in order to maximize the generated power output and its impact on other properties like voltage output.



### 1.1. Power Output Estimation

According to Faraday's law, the electromagnetic force,  $\varepsilon$  is estimated by the rate of change of the magnetic flux,  $\phi$ .

$$\varepsilon = -\frac{d\phi}{dt} \quad (1)$$

We can estimate the induced voltage,  $V_{\text{ind}}$  using Ohm's and Kirchoff's laws in a simple electrical circuit with known load resistance,  $R_{\text{load}}$  and internal resistance,  $R_{\text{internal}}$  respectively.

$$V_{\text{ind}} = \varepsilon \left( \frac{R_{\text{load}}}{R_{\text{load}} + R_{\text{internal}}} \right) \quad (2)$$

With  $V_{\text{ind}}$ ,  $R_{\text{load}}$  and  $R_{\text{internal}}$  is known, the power output,  $P_{\text{out}}$  of the harvesting system can be modelled and estimated by simulation using the Ohm's law.

$$P_{\text{out}} = \frac{V_{\text{ind}}^2}{R_{\text{load}} + R_{\text{internal}}} \quad (3)$$

### 1.2 Power-Optimizing Coils

The topology optimized coils which are cap look-like (see Figure 1 and Figure 2) could enhanced the generated power output more than 50% theoretically as proven through simulation [9]. The difficulties however lie in the realisation process whether technologically or financially.



**Figure 1.** Topology optimized cap-shaped coil [9]

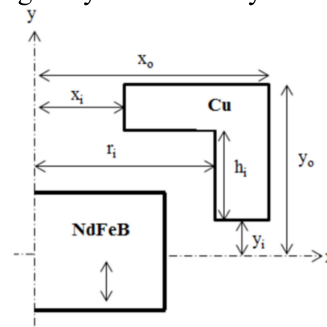


**Figure 2.** Geometrical properties of topology optimized coil [9]

### 1.3 Fill Factor

Filling factor,  $k_c$  concerns with the compactness of the wire winding in the desired size of coil which is useful to determine the quality of winding result. Basically we could derive it as the ratio of the area of the wire over the cross sectional area of the coil and the typical value is 0.6 [10].

$$k_c = \frac{\sum A_{\text{wire}}}{A_{\text{coil}}} \quad (4)$$

$A_{\text{wire}}$  is the cross-sectional area of the wire (usually made of copper) and  $A_{\text{coil}}$  is the cross-sectional area of the coil.

In order to facilitate the estimation process, the cross-sectional area of the coil is divided into two segments as shown in Figure 3.

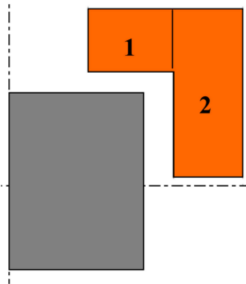


**Figure 3.** Cross-section of the coil

The cross-sectional area of the coil is divided into two parts,  $A_1$  and  $A_2$  as shown in Figure 3, where:

$$A_1 = \frac{1}{2}(D_i - D_{ii})(h_i) \quad (5)$$

$$A_2 = \frac{1}{2}(D_a - D_i)(h_a) \quad (6)$$

Using the information of resistivity and resistance of the copper wire, the number of winding of the coil can be estimated with:

$$N_1 = \frac{R}{\pi R' \left( D_{m1} + D_{m2} \left( \frac{A_2}{A_1} \right) \right)} \quad (7)$$

$$N_2 = \frac{R}{\pi R' \left( D_{m1} \left( \frac{A_2}{A_1} \right) + D_{m2} \right)} \quad (8)$$

where  $D_{m1}$  and  $D_{m2}$  are the diameter of section 1 and 2 respectively. The fill factor,  $k_c$  can be estimated using

$$k_c = \frac{\pi(N_1 + N_2)d_{wire}}{4(A_1 + A_2)} \quad (9)$$

## 2. Experiment Setup

We utilize the vibration generator (Data Physics GW-V4) together with a power amplifier (Data Physics PA30E) in the experiment. The shaker has the maximum amplitude and frequency capacities of 5.0mm and 14kHz respectively. Other than that OMRON Laser Reflective Sensor ZX-LD40 is used to monitor the frequency and amplitude of the generated vibration through the computer via a NI DAQ instrumentation. The schematic diagram of the experiment setup is shown in Figure 4.

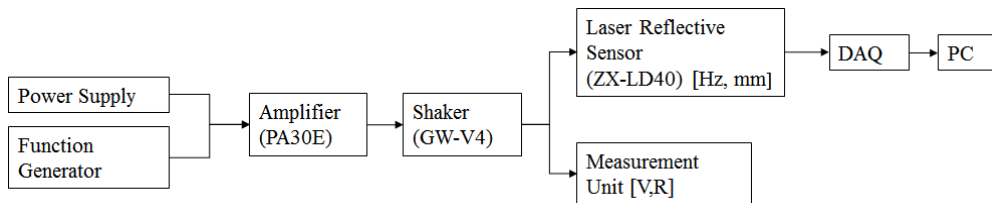


**Figure 4.** Experiment Setup Diagram

Besides it is also best to know the difference in the design of the coils for voltage and power output optimization. Therefore we have manufactured the coils of this form with variations in the dimensions as showed in

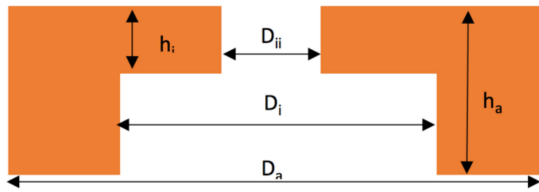


**Figure 5.** Dimensional parameters of the coils

These dimensional variations (see

**Table 1**) have been made to analyse the relationships between power output and voltage output with the geometrical properties of the proposed cap-shaped coils.

**Table 1.** Dimensional properties of the coils

| Coil | $D_a$ [mm] | $D_i$ [mm] | $D_{ii}$ [mm] | $H_a$ [mm] | $h_i$ [mm] |
|------|------------|------------|---------------|------------|------------|
| I    | 13.3       | 11.0       | 4.2           | 4.1        | 0.8        |
| II   | 12.8       | 11.0       | 4.0           | 4.8        | 1.7        |
| III  | 13.2       | 11.0       | 4.0           | 4.1        | 1.2        |
| IV   | 12.8       | 11.0       | 4.0           | 4.7        | 1.1        |
| V    | 12.2       | 11.2       | 4.2           | 4.5        | 1.2        |
| VI   | 13.5       | 11.0       | 4.3           | 4.4        | 1.3        |
| VII  | 12.9       | 11.0       | 4.0           | 4.7        | 1.1        |

### 3. Results and Discussion

The copper fill factor,  $k_c$  of the coils from Table 2 have been used to verify and compare the results from the simulation using the modelling of the electromagnetic vibration-based energy harvesting system in [9].

**Table 2.** Properties of the manufactured power-optimized coils

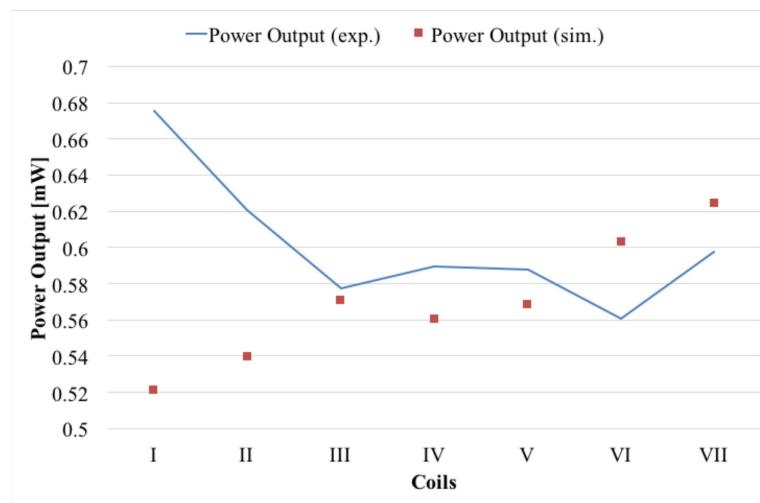
| Coil | Vol [cm <sup>3</sup> ] | Winding Number, n | Fill factor, $k_c$ |
|------|------------------------|-------------------|--------------------|
| I    | 1.08                   | 257               | 0.61               |
| II   | 1.13                   | 367               | 0.62               |
| III  | 1.13                   | 176               | 0.35               |
| IV   | 1.04                   | 259               | 0.57               |
| V    | 0.96                   | 209               | 0.57               |
| VI   | 1.19                   | 345               | 0.61               |
| VII  | 1.06                   | 297               | 0.63               |

Table 3 lists the boundary conditions for the simulation using software Matlab with FEMM.

**Table 3.** Boundary conditions for the Matlab-FEMM simulation

| Boundary condition         | Value                  |
|----------------------------|------------------------|
| Coercivity                 | 855000 [A/h]           |
| Relative permeability      | 1.049 [1]              |
| Remanence                  | 0.67 [T]               |
| Magnet height              | 6 [mm]                 |
| Magnet diameter            | 10 [mm]                |
| Copper wire diameter       | 150 [ $\mu$ m]         |
| Resistance per unit length | 13.6 [ $\Omega$ /m]    |
| Mechanical damping         | 0.10 [N/m/s]           |
| Excitation amplitude       | 10 [m/s <sup>2</sup> ] |
| Frequency                  | 100 [Hz]               |

From Figure 6 the results seem to diverge slightly for the coil I and II, whereas the rests proved the system modelling in [4] is dependable because the differences are small and negligible.



**Figure 6:** Comparison between experimental and simulation results for power output of the harvesting system

Figure 7 shows how cap-shaped coils able to generate power and voltage outputs with different sizes i.e. winding numbers. According to the Faraday's Law the bigger number of magnetic flux interception by the coils i.e. wires, the more voltage is being induced. This is perfectly proved in the diagram above where the coil with highest number of winding i.e. VII has the biggest amount of voltage output during the vibration. However, the optimal power output gives the opposite result where the coil with lowest winding number i.e. I generate most power.

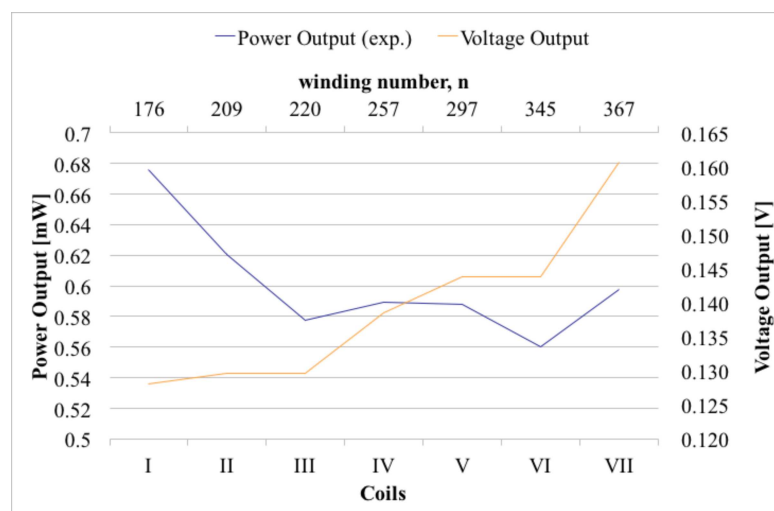


**Figure 7:** Power output and voltage output of the electromagnetic harvesting system using power-optimized coils

#### 4. References

- [1] E. Sardini and M. Serpelloni, "Sensors and Actuators A : Physical An efficient electromagnetic power harvesting device for low-frequency applications," *Sensors Actuators A. Phys.*, vol. 172, no. 2, pp. 475–482, 2011.
- [2] P. D. Mitcheson, T. C. Green, and E. M. Yeatman, "Power processing circuits for electromagnetic, electrostatic and piezoelectric inertial energy scavengers," pp. 1629–1635, 2007.

- [3] S. Roundy, P. K. Wright, and J. Rabaey, "A study of low level vibrations as a power source for wireless sensor nodes," *Comput. Commun.*, vol. 26, no. 11, pp. 1131–1144, 2003.
- [4] M. Zhu and E. Worthington, "Design and Testing of Piezoelectric Energy Harvesting Devices for Generation of Higher Electric Power for Wireless Sensor Networks," 2009.
- [5] S. Korla, R. A. Leon, I. N. Tansel, A. Yenilmez, A. Yapici, and M. Demetgul, "Design and testing of an efficient and compact piezoelectric energy harvester," *Microelectronics J.*, vol. 42, no. 2, pp. 265–270, 2011.
- [6] S. Boisseau, G. Despesse, and B. A. Seddik, "Electrostatic Conversion for Vibration Energy Harvesting," *Small-Scale Energy Harvest.*, pp. 1–39, 2012.
- [7] D. Spreemann, B. Folkmer, Y. Manoli, and I. Technology, "ARCHITECTURES FOR VIBRATION ENERGY HARVESTING DEVICES," pp. 257–260, 2008.
- [8] D. Spreemann and Y. Manoli, *Electromagnetic Vibration Energy Harvesting Devices: Architectures, Design, Modeling and Optimization*. 2012.
- [9] W. H. M. Isa and I. Ishak, "Analysis on the optimal geometrical parameters of topology power optimized coil based on a cylindrical magnet for vibration-based electromagnetic energy harvester," vol. 529, pp. 332–337, 2014.
- [10] M. P. Peter Spies, Loreto Mateu, *Handbook of Energy Harvesting Power Supplies and Applications*. Boca Raton, Florida: Pan Stanford Publishing, 2013.